

Pseudomonas aeruginosa biofilms perturb wound resolution and antibiotic tolerance in diabetic mice

Chase Watters · Katrina DeLeon · Urvish Trivedi ·
John A. Griswold · Mark Lyte · Ken J. Hampel ·
Matthew J. Wargo · Kendra P. Rumbaugh

Received: 9 August 2012 / Accepted: 6 September 2012 / Published online: 25 September 2012
© Springer-Verlag 2012

Abstract Diabetic patients are more susceptible to the development of chronic wounds than non-diabetics. The impaired healing properties of these wounds, which often develop debilitating bacterial infections, significantly increase the rate of lower extremity amputation in diabetic patients. We hypothesize that bacterial biofilms, or sessile communities of bacteria that reside in a complex matrix of exopolymeric material, contribute to the severity of diabetic wounds. To test this hypothesis, we developed an in vivo chronic wound, diabetic mouse model to determine the ability of the opportunistic pathogen, *Pseudomonas aeruginosa*, to cause biofilm-associated infections. Utilizing this model, we observed that diabetic mice with *P. aeruginosa*-infected chronic wounds displayed impaired bacterial clearing and wound closure in comparison with their non-diabetic littermates. While treating diabetic mice

with insulin improved their overall health, it did not restore their ability to resolve *P. aeruginosa* wound infections or speed healing. In fact, the prevalence of biofilms and the tolerance of *P. aeruginosa* to gentamicin treatment increased when diabetic mice were treated with insulin. Insulin treatment was observed to directly affect the ability of *P. aeruginosa* to form biofilms in vitro. These data demonstrate that the chronically wounded diabetic mouse appears to be a useful model to study wound healing and biofilm infection dynamics, and suggest that the diabetic wound environment may promote the formation of biofilms. Further, this model provides for the elucidation of mechanistic factors, such as the ability of insulin to influence antimicrobial effectiveness, which may be relevant to the formation of biofilms in diabetic wounds.

Keywords Diabetes · Chronic wounds · Biofilm · *Pseudomonas aeruginosa* · Antimicrobial tolerance · Insulin

C. Watters · K. DeLeon · U. Trivedi · J. A. Griswold ·
K. P. Rumbaugh (✉)
Department of Surgery, Texas Tech University Health
Sciences Center, 3601 4th Street, Lubbock, TX 79430,
USA
e-mail: kendra.rumbaugh@ttuhsc.edu

C. Watters · K. P. Rumbaugh
Department of Immunology and Molecular Microbiology,
Texas Tech University Health Sciences Center, Lubbock,
TX 79430, USA

M. Lyte
Department of Immunotherapeutics and Biotechnology,
Texas Tech University Health Sciences Center, Abilene,
TX 79601, USA

K. J. Hampel · M. J. Wargo
Department of Microbiology and Molecular Genetics,
University of Vermont College of Medicine, Burlington,
VT 05405, USA

Introduction

Diabetes affects 25.8 million people in the United States, or 8.3 % of the population, and 79 million more have pre-diabetes [1]. The complications of diabetes are varied, ranging from heart disease to blindness. Neuropathy occurs in up to 70 % of diabetics and contributes to the acquisition of chronic, slow-healing wounds, typically on the feet [1]. Approximately 15–25 % of diabetic patients will also develop foot ulceration during the course of their disease, many of which will necessitate lower extremity amputation [2]. In 2004, approximately 71,000 non-traumatic lower-limb amputations were performed on diabetics in the US [1]. The morbidity and mortality associated with lower

extremity amputation is significant, with up to 50 % of patients dying within the first 18 months, following amputation [2, 3] and up to 50 % of patients losing their contralateral extremity within 5 years [4, 5]. For these reasons, chronically infected diabetic foot ulcers are considered the most significant wound care problem in the United States and the world, and the exact cost of care for them is likely to be measured in the billions of dollars [6].

P. aeruginosa is one of the leading causes of infection in diabetic foot ulcers, and the increasing occurrence of multi-resistant strains is a major concern [7]. It has been hypothesized that one reason *P. aeruginosa* is so tolerant to antimicrobials is because of its ability to form biofilms, or structured communities of bacteria enclosed in a protective polysaccharide matrix [8]. Bacterial biofilms are the causative agents of several chronic diseases in humans and have been detected in human diabetic wounds [8–12]. It has been proposed that the presence of biofilms in wounds impedes the natural healing process for a variety of reasons including acting as a mechanical barrier, which impedes re-epithelization, stimulating a chronic state of inflammation, and providing protection from endogenous and exogenous antimicrobial agents [13–16]. However, very few of these hypotheses have been tested in vivo.

In the current study, we sought to develop a diabetic murine chronic wound model to investigate the role of *P. aeruginosa* biofilms in chronic wounds, and test the hypothesis that the diabetic wound environment promotes the formation and persistence of bacterial biofilms, resulting in delayed wound healing. Our data showed that the wounds of diabetic mice retained higher bacterial loads and healed more slowly than those of their non-diabetic littermates. *P. aeruginosa* imaged in diabetic wounds was more frequently aggregate-associated and displayed higher tolerance to gentamicin. Although insulin treatment appeared to improve the overall health of the mice, it did not greatly improve wound closure or bacterial clearance. In fact, diabetic mice on insulin treatment had more biofilm in their wounds, which displayed higher tolerance to gentamicin than in the untreated diabetic mice. Taken together, these data demonstrate that the chronically wounded diabetic mouse appears to be a useful model to study wound healing and biofilm infection dynamics, and suggest that the diabetic wound environment may promote the formation of biofilms.

Methods

Bacterial growth and inoculums

Pseudomonas aeruginosa strain PAO1 was grown in Luria–Bertani (LB) medium. Aliquots (50 µl) of overnight cultures were subcultured in fresh LB broth and grown at

37 °C for 4 h to an optical density of approximately 0.9 at 600 nm. A 100-µl aliquot of each culture was then pelleted, washed in phosphate-buffered saline (PBS) and serially diluted (tenfold serial dilutions) in PBS. A 100-µl aliquot of the 10^{-3} dilution (equivalent to approximately 10^4 CFU) was applied topically to the wound of each mouse. This dose has been empirically determined to cause an effective chronic infection in diabetic and non-diabetic mice [17]. The exact inoculum of each strain was determined by plating serial dilutions of the inoculum on LB and *Pseudomonas* isolation agar (Difco, Sparks, MD, USA).

Chronically wounded diabetic mouse model

A diabetic state was induced in wild-type 18–20 g female Swiss Webster mice (Charles River Laboratories) by the intraperitoneal injection of 250 mg/kg streptozotocin (STZ, Alexis Biochemicals, San Diego, CA, USA). STZ is toxic to the insulin-producing beta islet cells of the pancreas and is commonly used to induce a diabetic state in animal models [18]. Mice were deemed diabetic if their blood glucose levels were ≥ 20 mmol/L at 1-week post-STZ treatment. Mice were anesthetized, shaved, and administered a dorsal, full-thickness, 1.5×1.5 cm surgical excision wound. The wounds were covered with a transparent, semipermeable polyurethane dressing (OPSITE, Smith & Nephew, Hull, England) which allowed for daily inspection of the wound, wound size determination, topical application of bacteria onto the wound, and protection from other contaminating bacteria. Furthermore, the OPSITE dressing acted as a mechanical barrier to wound contraction, physically holding the wound open and resulting in a slow-healing wound. Approximately 10^4 CFU PAO1 was injected under the dressing, on top of the wound. Some groups of diabetic mice were treated subcutaneously with Humulin® N insulin (2 units, Eli Lilly, Indianapolis, IN, USA), given subcutaneously, per day.

Imaging aggregates in wound sections

Tissue was extracted from the wound/intact tissue interface at different time points and fixed in formalin, embedded in paraffin, sectioned, and stained with hematoxylin and eosin (H&E) to visualize the dermal architecture and bacteria. Slides were visualized by light microscopy (Eclipse 80i, Nikon Louisville, KY, USA), and images were captured and analyzed with the NIS elements program (version 3.00 SP7; Nikon, Japan). Fluorescent in situ hybridization (FISH) was performed on deparaffinized sections utilizing a Cy3-labeled oligonucleotide probe specific for the *P. aeruginosa* 16S ribosomal subunit, as previously described [19]. The *P. aeruginosa* glycocalyx was visualized by staining deparaffinized tissue sections with 50 µg/mL

of concanavalin A (ConA) fluorescein isothiocyanate (FITC) (MP Biomedicals, Solon, OH) for 5 min at room temperature in the dark as previously described [25]. The sections were then washed 3 times with PBS and incubated with DAPI (4',6'-diamidino-2-phenylindole) to stain DNA. Finally, the sections were fixed with ProLong Gold Antifade reagent (Molecular Probes, Eugene, OR, USA).

Gentamicin tolerance

Mice were given full-thickness surgical wounds and infected with PAO1 as described above. A sterile gauze pad was placed over the wound and then covered with an adhesive (OPSITE) dressing. At 4 days post-op, mice were euthanized and the gauze pads were removed from their wounds. The gauze pads were then cut in half and placed in sterile PBS or a 200 µg/mL gentamicin solution for 5 h. Gentamicin-treated gauze sections were then neutralized in Dey-Engley broth [20] for 10 min, after which they were placed into PBS and vigorously sonicated and vortexed. The resulting solutions were serially diluted and plated to determine the CFU/g of bandage. The CFU after gentamicin treatment was divided by the CFU from the untreated gauze section and multiplied by 100 to determine the percent of cells viable after treatment. Significant differences between groups were determined by ANOVA analysis, followed by the Tukey–Kramer multiple comparisons test (GraphPad Instat version 3.06, GraphPad Software).

Insulin effects on *P. aeruginosa* growth and biofilm formation in vitro

PAO1 was grown in LB broth at 37 °C overnight. From this overnight culture, a 100-µL sample was subcultured in 10 mL of serum-SAPI minimal medium. The serum-SAPI medium was prepared as previously described [21] and was composed as follows: 6.25 mM NH₄NO₃, 1.84 mM KH₂PO₄, 3.35 mM KCl, 1.01 mM MgSO₄, and 11.1 mM glucose, pH 7.5, supplemented with 30 % (v/v) adult bovine serum (Sigma, Poole, UK). Humulin® N insulin (Eli Lilly, Indianapolis, IN, USA) and purified recombinant human insulin (Prospec, Ness Ziona, Israel) were added to a final concentration of 200 nU, 200 µU, and 200 mU. Purified recombinant insulin was dissolved in 0.005 N HCl as per the manufacturer's instructions. H₂O and 0.005 N HCl were used as the vehicle controls. The cultures were then incubated at 37 °C for 24 h, and growth was monitored by the determination of CFU, every hour (from 1 to 10 h) and at 24 h.

To evaluate biofilm formation on Nunc Thermanox polymer plastic, cell-culture treated (TMX) coverslips (Nalge Nunc International, Rochester, NY, USA) and sterile 24-well polystyrene plates, containing serum-SAPI

medium, were inoculated with 10 µL of overnight cultures of PAO1. Humulin® N and purified recombinant human insulin were added to a final concentration of 200 nU, 200 µU, or 200 mU. For the denatured insulin experiments, Humulin® N insulin (200 nU, 200 µU, or 200 mU) was boiled for 5 min at 95 °C, cooled to 10 °C, and added to each well. The plates were covered and incubated at 37 °C for 4, 8, or 12 h with slow shaking on an orbital shaker. The crystal violet assay was then performed as previously described [22].

Microarray analysis

RNA from *P. aeruginosa* 8-h-old biofilms grown in serum-SAPI medium was prepared with the RNeasy kit (Qiagen), following manufacturer's instructions. Microarray analysis was performed on a *P. aeruginosa* PAO1 gene chip using raw oligonucleotide probes generated from each condition. Each sample was analyzed in duplicate ($N = 2$) and summarized in one probe intensity by the Vermont Genetics Network Microarray Facility using Affymetrix GCOS software. Information from multiple probes was combined to obtain a single measure of expression for each probe set and sample. Probe-level intensities were background-corrected, normalized, and summarized, and Robust Multichip Average (RMA) statistics were calculated for each probe set and sample as is implemented in Partek Genomic Suites®, version 6.6. Sample quality was assessed based on relative log expression (RLE) and normalized unscaled standard error (NUSE). To identify differentially expressed genes, linear modeling of sample groups was performed using ANOVA as implemented in Partek Genomic Suites. The magnitude of the response (fold change calculated using the least square mean) and the p value associated with each probe set, and binary comparison were calculated.

Results

Diabetic mice retained higher numbers of bacteria in their wounds and displayed delayed wound closure despite insulin treatment

STZ-treated mice have long been used to study the complications of diabetes [18, 23], and it is well documented that diabetic rodents and humans display impaired wound healing [24–26]. However, very few of these wound healing comparisons have been made in the context of infection. We utilized STZ-treated mice and their non-diabetic littermates to compare the rate of healing of *P. aeruginosa*-infected wounds. Mice were divided into three groups: non-diabetic, diabetic, or diabetic treated

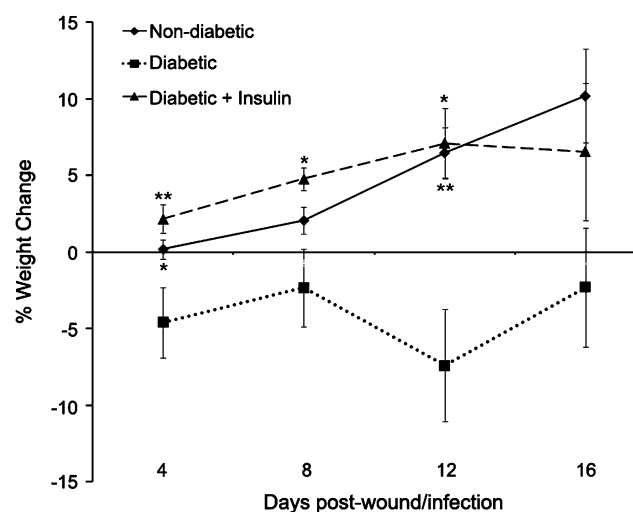


Fig. 1 Non-diabetic and diabetic mice treated with insulin gained more weight during the course of their infection than non-treated diabetic mice. Mice were weighed every 4 days and their percent body weight was calculated using the following equation: $(W_t - W_0)/W_0 \times 100$, where W_t is the weight on the day of observation and W_0 is the weight on the day of the surgery. One-way analysis of variance (ANOVA), followed by Tukey–Kramer multiple comparisons test was used to determine the difference between groups, * $p < 0.05$ and ** $p < 0.01$ ($n = 6$ –20/treatment group)

with insulin, administered full-thickness surgical excision wounds, which were covered with OPSITE dressings and infected with *P. aeruginosa*. This procedure generated a full-thickness, slow-healing wound, which remained open and chronically infected with high levels of *P. aeruginosa* for up to two and a half weeks in diabetic mice.

Over the 16 day experiment, the non-diabetic mice gained an average of 10 % of their body weight, while the diabetic mice lost an average of 2 % of their body weight (Fig. 1). Diabetic mice treated with insulin gained 6.6 % of their body weight and generally appeared much healthier than the untreated diabetic mice. As weight loss is one sign of a progressing disease or infection, these data suggest that the overall health of the untreated diabetic mice was considerably affected by the hyperglycemia and/or chronic *P. aeruginosa* infection.

On the day of surgery and at 4-day intervals, mice were anesthetized and weighed, and their wounds were photographed to determine the percent wound closure. Each wound was numbered and photographed adjacent to a ruler to ensure the results were not affected by the magnification of different pictures. The images were then analyzed in Adobe Photoshop to determine the wound area. The percent wound closure was determined using the following equation: $(A_0 - A_t)/A_0 \times 100$, where A_0 is the wound area on the day of the surgery, and A_t is the area of the wound on the day of observation. We observed that by day 4 post-infection the wounds of the non-diabetic mice had become

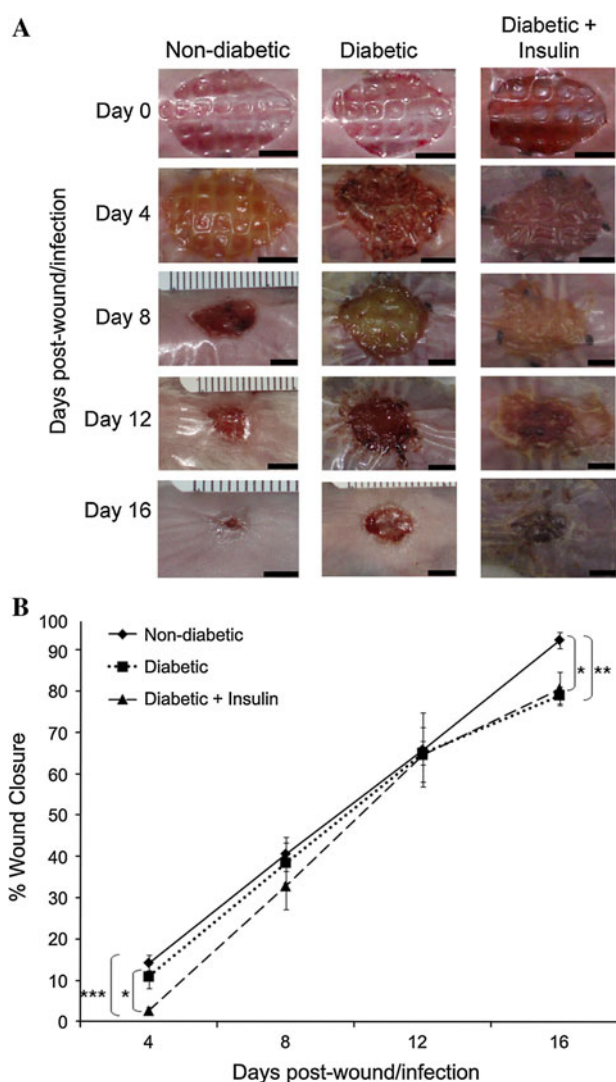


Fig. 2 Wound closure is delayed in diabetic mice. All wounds were photographed and measured every 4 days to assess wound closure (representative images are shown in **a**). The percent wound closure was determined using the following equation: $(A_0 - A_t)/A_0 \times 100$, where A_0 is the wound area on the day of the surgery and A_t is the area of the wound on the day of observation (**b**). One-way analysis of variance (ANOVA), followed by Tukey–Kramer multiple comparisons Test, * $p < 0.05$ and ** $p < 0.01$ ($n = 6$ –20/treatment group)

purulent, and although the percent wound closure was similar to that of diabetic mice (14 and 11 %, respectively), the wounds of the diabetic mice were dry and encrusted. The wounds of the diabetic mice treated with insulin appeared similar to those of the untreated diabetic mice (no purulent discharge); however, the percent wound closure for this group of mice was significantly lower (2.7 %) than the other two groups (Fig. 2a, b). By day 8, the purulence that was absent at day 4 in the wounds of the untreated and insulin-treated diabetic mice was evident (Fig. 2a), and percent wound closure was similar for all three groups. By

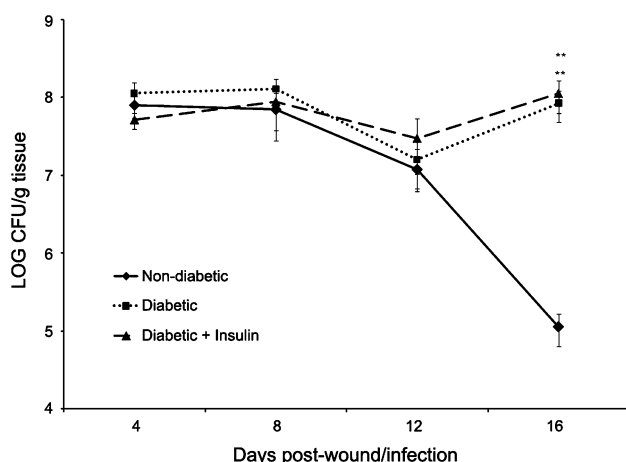


Fig. 3 Diabetic mice are impaired in their ability to clear *P. aeruginosa* from wounds. Wound tissue was harvested every 4 days and CFU were determined. One-way analysis of variance (ANOVA), followed by Kruskal–Wallis Test, ** $p < 0.01$

day 16, the wounds of the non-diabetic mice were almost completely closed (94 %), while the percent wound closure of the diabetic mice was significantly lower at 79 and 80 % for non-treated and insulin-treated, respectively.

The bacterial loads in the wounds were monitored every 4 days by euthanizing one group of mice and determining the CFU/g of wound tissue. In general, the bacterial load increased from the infecting dose of 10^4 CFU to approximately 10^{7-8} CFU/g tissue by day 4 in all three groups of mice (Fig. 3). However, by day 16, most of the non-diabetic wounds had closed and resolved the bacterial infection, while the wounds of the diabetic mice remained open and infected. Interestingly, the bacterial load in the wounds of the diabetic mice retained high levels of *P. aeruginosa* on day 16 despite insulin treatment. On average, it took another 4–6 days before the diabetic wounds closed completely and the bacterial loads decreased to those seen in non-diabetic mice (data not shown). These data suggested that while *P. aeruginosa* was able to infect the wounds of all three groups of mice equally, the non-diabetic mice may be more efficient at clearing the infection, which leads to faster healing. We also extracted liver and spleen tissue from the infected mice to determine whether the *P. aeruginosa* infection had spread systemically, but the organs remained uncolonized throughout the infection, indicating the *P. aeruginosa* remains localized to the wound bed (data not shown).

Pseudomonas aeruginosa aggregates were more prevalent in diabetic wounds and displayed an increased tolerance to gentamicin

It has been proposed that the presence of biofilms in wounds impedes the natural healing process for a variety of

reasons, including acting as a mechanical barrier that impedes re-epithelization, stimulating a chronic state of inflammation and providing protection from endogenous and exogenous antimicrobial agents [15, 16]. However, few of these theories have been tested in vivo. Thus, we sought to determine whether the delayed wound closure could be correlated with the presence of bacterial biofilm in the wound beds of our *P. aeruginosa*-infected mice. At each time point, tissue from the wound margin was excised, rinsed in sterile PBS, and processed for microscopy. Two hematoxylin and eosin-stained sections from each mouse were screened for the presence of bacterial aggregates (Fig. 4a–b), and a fluorescent in situ hybridization (FISH) probe specific for *P. aeruginosa* was used to localize highly infected areas (Fig. 4d). To visualize biofilm matrix interspersed between bacterial cells, we used concanavalin A fluorescein isothiocyanate (FITC), as previously described [27, 28]. ConA binds to mannose residues present in the glycocalyx. Although it is not specific for bacterial glycocalyx, we observed marked colocalization of ConA in areas with bacterial aggregates (Fig. 4e) versus uncolonized areas of the wound tissue (Fig. 4f).

Tissue sections were scored as biofilm positive or negative depending on the visualization of aggregates. *P. aeruginosa* aggregates were visualized by H&E staining and FISH exclusively within the wound bed and at the wound margin, indicating that the infections did not spread into the undamaged dermis. Aggregates were also visualized at all time points during the infection period, starting at four days post-infection, although in general, the aggregates from older wounds covered more surface area of the wound bed. As shown in Table 1, bacterial aggregates were visualized in only 3 sections from non-diabetic mice out of the 28 mice examined (11 %). This differed significantly from the 58 % of diabetic mice that were positive for aggregates (Chi squared with Yates correction equaled 11.241 with 1 degrees of freedom, $p = 0.0008$). Unexpectedly, mice treated with insulin had the highest frequency of aggregates at 67 %, which was also significantly increased from non-diabetic mice (Chi squared with Yates correction equaled 13.167 with 1 degrees of freedom, $p = 0.0003$).

One characteristic of biofilm-associated bacteria is their increased tolerance to antimicrobial agents [29]. Thus, we examined the tolerance of the bacteria in mouse chronic wounds to gentamicin, a commonly used antipseudomonal. As described above, mice were given full-thickness surgical wounds and infected with PAO1. These experiments differed only in that a sterile gauze pad was placed over the wound and then covered with an adhesive dressing. At 4 days post-infection, mice were euthanized and the gauze pads were removed from their wounds and treated with gentamicin. We detected a threefold increase (± 0.8 , $n = 8$)

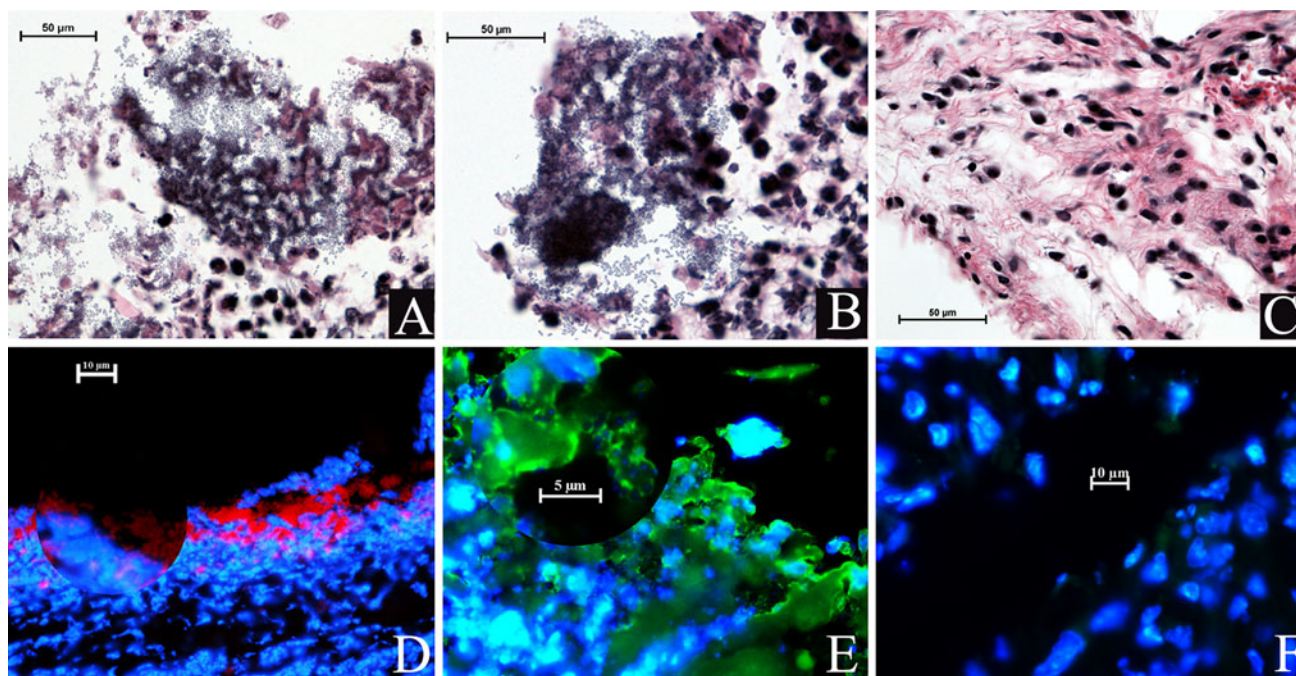


Fig. 4 Wound imaging reveals biofilm-associated bacterial aggregates. Tissue from the wound beds of 12-day diabetic (**a–b**) or non-diabetic (**c**) mice were fixed and imaged with H&E staining. Large aggregates of *P. aeruginosa* are visible in **a–b**, while section **c** is devoid of bacteria. A FISH probe, specific for *P. aeruginosa* (red), was used to localize highly infected areas from the wound beds of 12-day diabetic (**d**), while counterstaining with DAPI (blue) revealed

host cell nuclei. Con A-FITC was used to visualize the glycocalyx (green) around bacteria in the wound bed of a 12-day diabetic, and counterstaining with DAPI revealed bacterial cell nuclei within the matrix (blue areas in magnified area) (**e**). An area of the same tissue section, stained with ConA, but with no bacteria, is shown in (**f**) as a negative control (color figure online)

Table 1 Prevalence of *P. aeruginosa* biofilm in wounds of non-diabetic and diabetic mice

	Biofilm positive mice/total number of mice	0–8 Day	9–16 Day
Non-diabetic	3/28 (11 %)	2	1
Diabetic	14/24 (58 %)	7	7
Diabetic + insulin	12/18 (67 %)	3	9

in the number of *P. aeruginosa* that were still viable after gentamicin treatment from the wounds of diabetic mice compared to non-diabetic mice. More strikingly, we observed a ninefold increase (± 3.8 , $n = 8$, $p < 0.05$) in the number of *P. aeruginosa* that remained viable in the insulin-treated diabetic mice in comparison with non-diabetic mice. When bacteria were removed from the wound by swabbing and returned to their planktonic state, they were susceptible to 1.563 $\mu\text{g/mL}$ of gentamicin (data not shown), indicating that the increased tolerance was transient and dependent on the wound environment, which is consistent with biofilm-associated tolerance rather than genetic changes generating resistance. Furthermore, the increased antibiotic tolerance of bacteria in wounds was consistent with the higher numbers of biofilm positive

tissue sections that we visualized from diabetic mice (Table 1) and supported our hypothesis that the diabetic wound environment promotes the formation of biofilms. These data also demonstrated that insulin treatment, either directly or indirectly, further promoted *P. aeruginosa* biofilm formation and antibiotic tolerance in wounds. Thus, we next sought to examine if insulin directly affected *P. aeruginosa*.

In vitro effect of insulin on *P. aeruginosa*

We first tested whether insulin treatment increased the growth of planktonic *P. aeruginosa*, to examine the possibility that *P. aeruginosa* simply grew faster in the wounds of insulin-treated mice and thus was able to establish a foothold quicker within the wound bed. The only published studies examining the direct interactions between insulin and *P. aeruginosa* showed that in the presence or absence of glucose, insulin at microunits decreased *P. aeruginosa* planktonic growth [30]; however, the investigators of this study used Humulin® which contains an antimicrobial (metacresol) that could account for the inhibition of growth [31]. For our investigations, we used two forms of insulin: Humulin® and purified recombinant human insulin which does not contain (m-cresol). The circulating levels of free

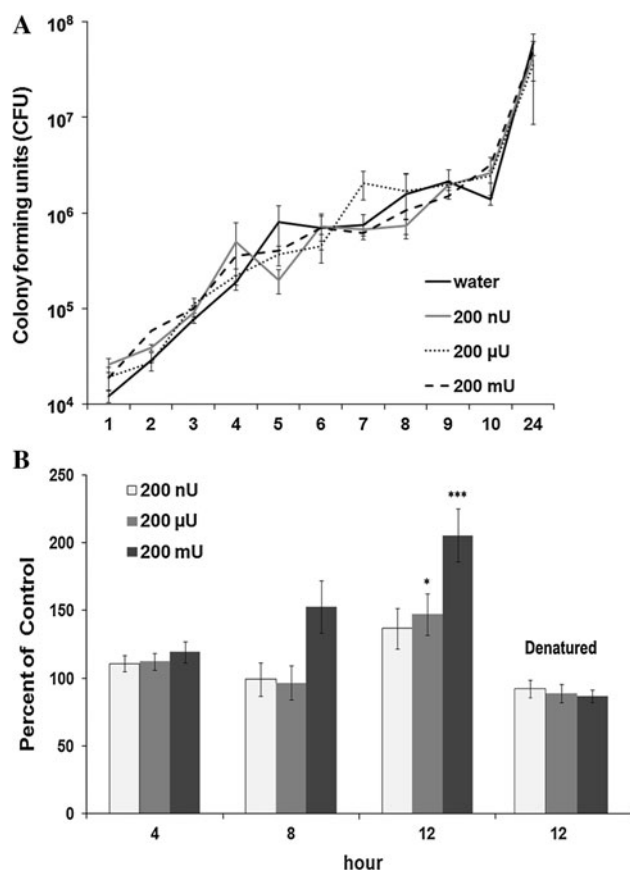


Fig. 5 Insulin promotes *P. aeruginosa* biofilm formation in vitro. *P. aeruginosa* was grown in serum-SAPI medium in the presence of a vehicle control, 200 nU, μ U or mU Humulin® and/or 200 nU, μ U or mU heat-denatured Humulin® and planktonic growth (a) or biofilm formation (b) was monitored. One-way analysis of variance (ANOVA), followed by Tukey–Kramer multiple comparisons test * $p < 0.05$ and *** $p < 0.001$

insulin range from 25 to 250 μ U/mL [32], and blood glucose levels can fluctuate between 200 and 651 mg/dL [33]. Similarly, the mice in our study were treated with 2 U of insulin (Humulin®) per day and their blood glucose levels fluctuated from 40 to 540 mg/dL, compared to non-treated diabetic mice whose blood glucose levels fluctuated from 326 to 500 mg/dL, and non-diabetic mice whose blood glucose levels were consistently under 100 mg/dL. In an attempt to mimic these conditions in vitro, we grew planktonic cultures of *P. aeruginosa* in a serum-SAPI minimal medium that more closely mimics the in vivo milieu [21], with glucose concentrations of 11.1 mM as this mimics the basal hyperglycemic levels observed in diabetic patients (200 mg/dL = 11.1 mM/L) [34]. We added insulin at concentrations ranging from 200 nU to 200 mU [30, 32, 35] or H₂O as a control. We did not observe any changes in the growth of *P. aeruginosa* in response to Humulin® (Fig. 5a) or purified insulin (not shown) when compared to a vehicle control.

We next tested whether insulin affected the ability of *P. aeruginosa* to form biofilms on plastic coverslips under the same growth conditions as described above. We examined biofilm formation at early time points (4–12 h), with both forms of insulin, based on the rationale that biofilms may form earlier in insulin-treated mice. Significantly, more biofilm was formed on coverslips when the culture media was supplemented with 200 μ U and 200 mU of Humulin® (Fig. 5b) and purified insulin (not shown). However, when we heat-denatured Humulin® we did not see the same increase in biofilm biomass at the 12-h time point (Fig. 5b). Tolerance assays were also performed on biofilm cells grown on gauze under these conditions for 12 h, and we observed a 1.8-fold increase (± 0.26 , $n = 8$, $p < 0.05$) in the number of cells that survived gentamicin treatment when the cells were exposed to 200 μ U Humulin®. These data demonstrate that active, but not denatured, insulin enhances *P. aeruginosa* biofilm formation, and thus gentamicin tolerance, in vitro.

To examine whether insulin directly influenced the expression of *P. aeruginosa* biofilm-associated factors, we performed a microarray analysis on cells grown under the same growth conditions used above for 8 h and supplemented with 200 μ U Humulin®, 200 μ U heat-denatured Humulin® or water as a control. Table 2 lists the genes whose transcription was significantly altered by active versus heat-denatured Humulin®. Very few changes were indicated by the microarray data, and the changes that were noted were very small, leading us to speculate that either these small differences are indicative of protein folding or metabolic changes that lead to increased biofilm formation, or more likely that they are unrelated markers of non-transcriptional changes taking place due to interaction with the insulin. Additional phenotypic assays, performed to determine whether insulin affected the production of elastase, pyocyanin, pyoverdine, or the generation of quorum signals, yielded no significant differences between insulin-treated cells and controls (not shown).

Discussion

While there is little doubt that biofilms are present in wounds, controversy remains whether or not they affect healing or immune responses. In a recent editorial, Singh and Barbul wrote, ‘All open wounds are colonized by microorganisms, and chronic wounds especially so. Once the bacterial burden reaches a certain level, the healing process becomes impaired, but the question remains whether bacterial colonization is a causative factor in the failure of chronic wounds to heal and whether the biofilm state contributes to this pathology’ [36]. Experimental data regarding the role of biofilms in wound healing are also

Table 2 Changes detected in microarray analysis of *P. aeruginosa* exposed to active (I) versus heat-denatured (DI) insulin

Gene symbol	Gene title	<i>p</i> value (I vs. DI)	Fold change (I vs. DI)
lldP	L-lactate permease	0.0291047	3.34626
hslU	Heat shock protein HslU	0.013699	2.34357
hslV	Heat shock protein HslV	0.00320011	2.32958
htpG	Heat shock protein HtpG	0.0475272	2.18458
grpE	Heat shock protein GrpE	0.0183096	2.16998

inconclusive. For example, Kanno et al. [37] demonstrated that although *P. aeruginosa* formed biofilms in the wounds of rats, infection did not correlate with a delay in re-epithelialization. On the other hand, Schierle et al. [38] reported that both *Staphylococcus aureus* and *Staphylococcus epidermidis* biofilms slowed wound re-epithelialization in a mouse full-thickness excision punch wound. While several groups have now reported on the correlation between the presence of biofilm in wounds and slower healing rates [38–42], to our knowledge, there have been no systematic empirical studies comparing the efficacy of ‘antibiofilm’ therapeutics to classical treatments in relation to wound healing. It should be noted, however, that utilizing ‘biofilm-based wound care’ management strategies designed to suppress and eradicate biofilms, reportedly led to a significantly higher healing rate in patients being treated at the Southwest Regional Wound Care Center in Lubbock, Texas [43].

The goals of our study were to utilize a mouse model to determine whether *P. aeruginosa* formed biofilms more prevalently in diabetic wounds and if these biofilms contributed to impaired wound healing. We used STZ to induce diabetes in otherwise healthy, outbred mice. Mimicking type I diabetes, STZ destroys the beta islet cells of the pancreas and thus STZ-treated mice are unable to produce insulin, become severely hyperglycemic, and typically do not gain weight, reminiscent of human type 1 diabetes [44]. The STZ-treated diabetic rodent has long been used as a model to study aspects of diabetes, including impaired wound healing, and STZ-treated mice and rats have significantly decreased wound tensile strength, collagen formation, granulation tissue formation, and neovascularization in comparison with controls [24–26]. However, the deficiencies seen in the healing of STZ-treated mice versus control mice are not nearly as profound as those seen in genetically diabetic db/db mice, which have a spontaneous mutation in the leptin receptor that results in insulin tolerance, hyperglycemia, and excessive weight gain, reminiscent of human type 2 diabetes [26]. In the context of healing infected wounds, the disparity between these two models may be even more apparent. For example, Holder et al. studied wound closure in C57BL/KsJ-db/db mice given similar-sized, full-thickness wounds, infected with the

same dose of *P. aeruginosa* [17] as the present study. In comparison with their wild-type littermates who displayed 90 % wound closure by day 15, the wound areas of the db/db mice actually increased by 100 % by day 12. Interestingly, while the sizes of these wounds differed dramatically between diabetic versus non-diabetic mice, the bacterial load for both groups remained relatively constant (10^{10} and 10^9 CFU/mL, respectively) for days 1–7. Holder et al. also demonstrated that wound closure was impaired by *P. aeruginosa* infection in both non-diabetic and diabetic mice; however, the impairment was dramatically more severe in infected diabetic mice [17]. The data presented in the present study clearly demonstrate that bacterial infection, at least by *P. aeruginosa*, inhibits healing in mice. We also utilized db/db mice in our studies and saw similar results as did Holder et al. (data not shown). However, because db/db mice displayed severe innate healing delays, regardless of infection or the presence of biofilms, and our goal was to study the role of biofilms in healing, we decided to perform the remainder of the study with STZ-treated mice.

We observed significant differences in wound closure between non-diabetic and diabetic mice occurring early in the infection (day 4) and late (day 16). We also observed that the bacterial burden in the wounds of non-diabetic mice decreased dramatically in comparison with the diabetic mice as their wounds reached complete closure. We also observed that biofilms were much more prevalent in diabetic wounds, supporting our hypothesis that the diabetic wound environment promotes the formation and persistence of bacterial biofilms. These biofilms were present at every time point examined; however, the area of the wound bed covered by biofilm appeared to increase with time, and we detected biofilm in only one non-diabetic mouse at a late time point. These data were consistent with our CFU data, suggesting that most of the non-diabetic mice had cleared the infection by week two. We also observed that the bacteria in diabetic wounds were more tolerant to gentamicin, which could be due to the increased prevalence of biofilms.

Our most surprising observations were seen among the diabetic mice on insulin treatment. These data are particularly relevant because this group of mice more accurately reflects the clinical picture of most diabetic patients who

would be on insulin therapy to control their disease. Although insulin treatment improved the overall health of mice, it did not improve wound closure or bacterial clearance. Unexpectedly, more biofilm was observed in the wounds of insulin-treated diabetic mice, which correlated with higher antibiotic tolerance. To our knowledge, no studies examining the effects of systemic insulin treatment on healing in the context of chronic wound *P. aeruginosa* infections have been reported. Insulin therapy has been explored in chronic lung infections of diabetic cystic fibrosis patients, and while this therapy decreased *H. influenzae* and *S. pneumoniae* bacterial load, *P. aeruginosa* growth remained unchanged [45]. It is interesting to note that in burned rats a low dose of insulin treatment was shown to decrease the systemic dissemination of *P. aeruginosa* [46], and intensive insulin therapy in severely burned patients has been shown to reduce sepsis [47]. These studies could suggest that insulin treatment for burn wounds decreases the acute, planktonic growth of *P. aeruginosa* in favor of a chronic, biofilm mode of growth. Taken together, these previous reports and our in vivo data raise the possibility that insulin treatment, either directly or indirectly, affects *P. aeruginosa* resulting in more biofilm formation.

We observed that while insulin did not directly affect *P. aeruginosa*'s growth, it did promote biofilm formation and increased gentamicin tolerance in vitro and these effects were negated when cells were exposed to heat-denatured insulin. While only small changes in gene expression were observed after *P. aeruginosa* was exposed to active insulin in vitro, the mRNA levels of an L-lactate permease (lldP) and several heat shock proteins were increased above twofold. Interestingly, L-lactate permease is involved in the transport of small molecules and sugar metabolism and has been identified to play a role in biofilm formation in *Bacillus subtilis* [48]; although, its role in *P. aeruginosa* biofilm formation has not been reported. Our next step in this study will be to determine whether a *P. aeruginosa* lldP-deficient strain displays increased biofilm formation and gentamicin tolerance in response to insulin.

While (200 μ M to 200 mM) levels of insulin did affect *P. aeruginosa* biofilm formation in vitro, we cannot be sure that these levels are achieved in wounds. Information regarding the levels that insulin can reach in the periphery is scarce; however, 90 s after injecting 400 ng of insulin into the vena cava of rats, Pelerinelli et al. [49] detected approximately 40–70 μ U/mL in the periphery (skin). If we assumed the same was true for our mice, which were treated with approximately 69 μ g of insulin (equal to 2 U), we would expect a peripheral insulin concentration around 8 mU, a concentration which clearly affects *P. aeruginosa* directly in vitro. It is also possible that the observed increases in biofilm and tolerance seen in vivo could also be an indirect effect of insulin's action on the immune

status of the mice. Insulin treatment may modulate the immune response in a manner that favors infection and/or biofilm formation (e.g., delaying initial inflammation) [50–53]. Consequently, future studies will focus on how changes in the immune status of the diabetic host changes in response to insulin treatment and whether these immune changes support biofilm formation.

Acknowledgments This study was supported by American Diabetes Association research grant #1-08-RA-165 to KPR. KD and UT were supported by a Howard Hughes Medical Institute grant through the Undergraduate Science Education Program to Texas Tech University. MJW was supported by a grant to the Vermont Center for Immunology and Infectious Disease from the National Center for Research Resources (5P20RR021905-07).

References

- Centers for Disease Control and Prevention (2011) National diabetes fact sheet: national estimates and general information on diabetes and prediabetes in the United States, 2011. US Department of Health and Human Services, Centers for Disease Control and Prevention, Atlanta
- Reiber GE (1996) The epidemiology of diabetic foot problems. *Diabet Med* 13(Suppl 1):S6–11
- Ohsawa S, Inamori Y, Fukuda K, Hirotsuji M (2001) Lower limb amputation for diabetic foot. *Arch Orthop Trauma Surg* 121(4): 186–190
- Ebskov B, Josephsen P (1980) Incidence of reamputation and death after gangrene of the lower extremity. *Prosthet Orthot Int* 4(2):77–80
- Armstrong DG, Lavery LA, Harkless LB, Van Houtum WH (1997) Amputation and reamputation of the diabetic foot. *J Am Podiatr Med Assoc* 87(6):255–259
- Cunningham AB (2006) *Biofilms: The Hypertextbook*. Montana State University, Bozeman
- Yoga R, Khairul A, Sunita K, Suresh C (2006) Bacteriology of diabetic foot lesions. *Med J Mala* 61 Suppl A:14–16
- Costerton JW, Stewart PS, Greenberg EP (1999) Bacterial biofilms: a common cause of persistent infections. *Science* 284(5418):1318–1322
- Donlan RM, Costerton JW (2002) Biofilms: survival mechanisms of clinically relevant microorganisms. *Clin Microbiol Rev* 15(2):167–193
- Ehrlich GD, Veeh R, Wang X, Costerton JW, Hayes JD, Hu FZ, Daigle BJ, Ehrlich MD, Post JC (2002) Mucosal biofilm formation on middle-ear mucosa in the chinchilla model of otitis media. *JAMA* 287(13):1710–1715
- Singh PK, Schaefer AL, Parsek MR, Moninger TO, Welsh MJ, Greenberg EP (2000) Quorum-sensing signals indicate that cystic fibrosis lungs are infected with bacterial biofilms. *Nature* 407(6805):762–764
- Slusher MM, Myrvik QN, Lewis JC, Gristina AG (1987) Extended-wear lenses, biofilm, and bacterial adhesion. *Arch Ophthalmol* 105(1):110–115
- Edwards R, Harding KG (2004) Bacteria and wound healing. *Curr Opin Infect Dis* 17(2):91–96
- James GA, Swogger E, Wolcott R, Pulcini E, Secor P, Sestrich J, Costerton JW, Stewart PS (2008) Biofilms in chronic wounds. *Wound Repair Regen* 16(1):37–44
- Wolcott RD, Ehrlich GD (2008) Biofilms and chronic infections. *JAMA* 299(22):2682–2684

16. Bjarnsholt T, Kirketerp-Moller K, Jensen PO, Madsen KG, Phipps R, Krogfelt K, Hoiby N, Givskov M (2008) Why chronic wounds will not heal: a novel hypothesis. *Wound Repair Regen* 16(1):2–10. doi:[10.1111/j.1524-475X.2007.00283.x](https://doi.org/10.1111/j.1524-475X.2007.00283.x)
17. Holder IA, Brown RL, Greenhalgh DG (1997) Mouse models to study wound closure and topical treatment of infected wounds in healing-impaired and normal healing hosts. *Wound Repair Regen* 5:198–204
18. Tesch GH, Allen TJ (2007) Rodent models of streptozotocin-induced diabetic nephropathy. *Nephrology (Carlton)* 12(3):261–266. doi:[10.1111/j.1440-1797.2007.00796.x](https://doi.org/10.1111/j.1440-1797.2007.00796.x)
19. Schaber JA, Triffo WJ, Suh SJ, Oliver JW, Hastert MC, Griswold JA, Auer M, Hamood AN, Rumbaugh KP (2007) *Pseudomonas aeruginosa* forms biofilms in acute infection independent of cell-to-cell signaling. *Infect Immun* 75(8):3715–3721
20. Wolcott RD, Rumbaugh KP, James G, Schultz G, Phillips P, Yang Q, Watters C, Stewart PS, Dowd SE (2010) Biofilm maturity studies indicate sharp debridement opens a time-dependent therapeutic window. *J Wound Care* 19(8):320–328
21. Lyte M, Ernst S (1992) Catecholamine induced growth of gram negative bacteria. *Life Sci* 50(3):203–212
22. Hammond A, Dertien J, Colmer-Hamood JA, Griswold JA, Hamood AN (2010) Serum inhibits *P. aeruginosa* biofilm formation on plastic surfaces and intravenous catheters. *J Surg Res* 159(2):735–746. doi:[10.1016/j.jss.2008.09.003](https://doi.org/10.1016/j.jss.2008.09.003)
23. Shen X, Bornfeldt KE (2007) Mouse models for studies of cardiovascular complications of type 1 diabetes. *Ann N Y Acad Sci* 1103:202–217. doi:[10.1196/annals.1394.004](https://doi.org/10.1196/annals.1394.004)
24. Spanheimer RG, Umpierrez GE, Stumpf V (1988) Decreased collagen production in diabetic rats. *Diabetes* 37(4):371–376
25. Covington DS, Xue H, Pizzini R, Lally KP, Andrassy RJ (1993) Streptozotocin and alloxan are comparable agents in the diabetic model of impaired wound healing. *Diabetes Res* 23(2):47–53
26. Jt Michaels, Churgin SS, Blechman KM, Greives MR, Aarabi S, Galiano RD, Gurtner GC (2007) db/db mice exhibit severe wound-healing impairments compared with other murine diabetic strains in a silicone-splinted excisional wound model. *Wound Repair Regen* 15(5):665–670. doi:[10.1111/j.1524-475X.2007.00273.x](https://doi.org/10.1111/j.1524-475X.2007.00273.x)
27. Kania RE, Lamers GE, Vonk MJ, Huy PT, Hiemstra PS, Bloembergen GV, Grote JJ (2007) Demonstration of bacterial cells and glycocalyx in biofilms on human tonsils. *Arch Otolaryngol Head Neck Surg* 133(2):115–121. doi:[10.1001/archotol.133.2.115](https://doi.org/10.1001/archotol.133.2.115)
28. Akiyama H, Huh WK, Yamasaki O, Oono T, Iwatsuki K (2002) Confocal laser scanning microscopic observation of glycocalyx production by *Staphylococcus aureus* in mouse skin: does *S. aureus* generally produce a biofilm on damaged skin? *Br J Dermatol* 147(5):879–885
29. Anderson GG, O'Toole GA (2008) Innate and induced resistance mechanisms of bacterial biofilms. *Curr Top Microbiol Immunol* 322:85–105
30. Plotkin BJ, Viselli SM (2000) Effect of insulin on microbial growth. *Curr Microbiol* 41(1):60–64
31. Jeromson S, Keig P, Kerr K (1999) Interaction of insulin and *Burkholderia cepacia*. *Clin Microbiol Infect* 5(7):439–442
32. Hayford JT, Thompson RG (1982) Free and total insulin integrated concentrations in insulin dependent diabetes. *Metabolism* 31(4):387–397. doi:[10.1002-0495\(82\)90116-0](https://doi.org/10.1002-0495(82)90116-0)
33. Hirose H, Takayama T, Hozawa S, Hibi T, Saito I (2011) Prediction of metabolic syndrome using artificial neural network system based on clinical data including insulin resistance index and serum adiponectin. *Comput Biol Med* 41(11):1051–1056. doi:[10.1016/j.combiomed.2011.09.005](https://doi.org/10.1016/j.combiomed.2011.09.005)
34. Yang M, Guo Q, Zhang X, Sun S, Wang Y, Zhao L, Hu E, Li C (2009) Intensive insulin therapy on infection rate, days in NICU, in-hospital mortality and neurological outcome in severe traumatic brain injury patients: a randomized controlled trial. *Int J Nurs Stud* 46(6):753–758. doi:[10.1016/j.ijnurstu.2009.01.004](https://doi.org/10.1016/j.ijnurstu.2009.01.004)
35. Woods DE, Jones AL, Hill PJ (1993) Interaction of insulin with *Pseudomonas pseudomallei*. *Infect Immun* 61(10):4045–4050
36. Singh VA, Barbul A (2008) Bacterial biofilms in wounds. *Wound Repair Regen* 16(1):1. doi:[10.1111/j.1524-475X.2007.00349.x](https://doi.org/10.1111/j.1524-475X.2007.00349.x)
37. Kanno E, Toriyabe S, Zhang L, Imai Y, Tachi M (2009) Biofilm formation on rat skin wounds by *Pseudomonas aeruginosa* carrying the green fluorescent protein gene. *Exp Dermatol*. doi:[10.1111/j.1600-0625.2009.00931.x](https://doi.org/10.1111/j.1600-0625.2009.00931.x)
38. Schierle CF, De la Garza M, Mustoe TA, Galiano RD (2009) Staphylococcal biofilms impair wound healing by delaying reepithelialization in a murine cutaneous wound model. *Wound Repair Regen* 17(3):354–359. doi:[10.1111/j.1524-475X.2009.00489.x](https://doi.org/10.1111/j.1524-475X.2009.00489.x)
39. Seth AK, Geringer MR, Gurjala AN, Hong SJ, Galiano RD, Leung KP, Mustoe TA (2012) Treatment of *Pseudomonas aeruginosa* biofilm-infected wounds with clinical wound care strategies: a quantitative study using an in vivo rabbit ear model. *Plast Reconstr Surg* 129(2):262e–274e. doi:[10.1097/PRS.0b013e31823aeb3b](https://doi.org/10.1097/PRS.0b013e31823aeb3b)
40. Dalton T, Dowd SE, Wolcott RD, Sun Y, Watters C, Griswold JA, Rumbaugh KP (2011) An in vivo polymicrobial biofilm wound infection model to study interspecies interactions. *PLoS ONE* 6(11):e27317. doi:[10.1371/journal.pone.0027317](https://doi.org/10.1371/journal.pone.0027317)
41. Gurjala AN, Geringer MR, Seth AK, Hong SJ, Smeltzer MS, Galiano RD, Leung KP, Mustoe TA (2011) Development of a novel, highly quantitative in vivo model for the study of biofilm-impaired cutaneous wound healing. *Wound Repair Regen* 19(3):400–410. doi:[10.1111/j.1524-475X.2011.00690.x](https://doi.org/10.1111/j.1524-475X.2011.00690.x)
42. Zhao G, Hochwalt PC, Usui ML, Underwood RA, Singh PK, James GA, Stewart PS, Fleckman P, Olerud JE (2010) Delayed wound healing in diabetic (db/db) mice with *Pseudomonas aeruginosa* biofilm challenge: a model for the study of chronic wounds. *Wound Repair Regen* 18(5):467–477
43. Wolcott RD, Rhoads DD (2008) A study of biofilm-based wound management in subjects with critical limb ischaemia. *J Wound Care* 17(4):145–148, 150–142, 154–145
44. Wu K, Kah, Y. (2008) Streptozotocin-induced diabetic models in mice and rats. *Curr Protoc Pharmacol UNIT* 5.47 doi:[10.1002/0471141755.ph0547s40](https://doi.org/10.1002/0471141755.ph0547s40)
45. Lannig S, Thorsteinsson B, Nerup J, Koch C (1994) Diabetes mellitus in cystic fibrosis: effect of insulin therapy on lung function and infections. *Acta Paediatr* 83(8):849–853
46. Gauglitz GG, Toliver-Kinsky TE, Williams FN, Song J, Cui W, Herndon DN, Jeschke MG (2010) Insulin increases resistance to burn wound infection-associated sepsis. *Crit Care Med* 38(1):202–208. doi:[10.1097/CCM.0b013e3181b43236](https://doi.org/10.1097/CCM.0b013e3181b43236)
47. Jeschke MG, Kulp GA, Kraft R, Finnerty CC, Mlcak R, Lee JO, Herndon DN (2010) Intensive insulin therapy in severely burned pediatric patients: a prospective randomized trial. *Am J Respir Crit Care Med* 182(3):351–359. doi:[10.1164/rccm.201002-0190OC](https://doi.org/10.1164/rccm.201002-0190OC)
48. Chai Y, Kolter R, Losick R (2009) A widely conserved gene cluster required for lactate utilization in *Bacillus subtilis* and its involvement in biofilm formation. *J Bacteriol* 191(8):2423–2430. doi:[10.1128/JB.01464-08](https://doi.org/10.1128/JB.01464-08)
49. Pelegrielli FF, Thirone AC, Gasparetti AL, Araujo EP, Velloso LA, Saad MJ (2001) Early steps of insulin action in the skin of intact rats. *J Invest Dermatol* 117(4):971–976. doi:[10.1046/j.0022-202x.2001.01473.x](https://doi.org/10.1046/j.0022-202x.2001.01473.x)
50. Dandona P, Aljada A, Mohanty P, Ghanim H, Hamouda W, Assian E, Ahmad S (2001) Insulin inhibits intranuclear nuclear factor kappaB and stimulates IkappaB in mononuclear cells in obese subjects: evidence for an anti-inflammatory effect? *J Clin Endocrinol Metab* 86(7):3257–3265

51. Dandona P, Chaudhuri A, Mohanty P, Ghanim H (2007) Anti-inflammatory effects of insulin. *Curr Opin Clin Nutr Metab Care* 10(4):511–517. doi:[10.1097/MCO.0b013e3281e38774](https://doi.org/10.1097/MCO.0b013e3281e38774)
52. Ghanim H, Mohanty P, Deopurkar R, Sia CL, Korzeniewski K, Abuaysheh S, Chaudhuri A, Dandona P (2008) Acute modulation of toll-like receptors by insulin. *Diabetes Care* 31(9):1827–1831. doi:[10.2337/dc08-0561](https://doi.org/10.2337/dc08-0561)
53. Kidd LB, Schabbauer GA, Luyendyk JP, Holscher TD, Tilley RE, Tencati M, Mackman N (2008) Insulin activation of the phosphatidylinositol 3-kinase/protein kinase B (Akt) pathway reduces lipopolysaccharide-induced inflammation in mice. *J Pharmacol Exp Ther* 326(1):348–353. doi:[10.1124/jpet.108.138891](https://doi.org/10.1124/jpet.108.138891)